On the lateral crystal growth of laser irradiated NiTi thin films

A. J. Birnbaum,[1,a)] Y. Lawrence Yao,[1] U.-J. Chung,[2] James. S. Im,[2] X. Huang,[3] and A. G. Ramirez[3]
[1]*Department of Mechanical Engineering, Columbia University, New York, New York 10027, USA*
[2]*Department of Applied Physics and Applied Mathematics, Program in Materials Science, Columbia University, New York, New York 10027, USA*
[3]*Department of Mechanical Engineering, Yale University, New Haven, Connecticut 06511, USA*

(Received 5 January 2009; accepted 15 April 2009; published online 2 July 2009)

This letter demonstrates the ability to induce laterally grown, large-aspect crystals via pulsed, melt-mediated laser crystallization in NiTi thin films. Sputter-deposited 200 nm NiTi films were pulse irradiated utilizing a homogenized 308 nm excimer beam over a series of varying incident laser energy densities. Solidification occurred via two distinct pathways: nucleation and growth occurred away from the boundary of irradiation, while lateral growth of unmelted seeds into the undercooled melt developed at the boundary of irradiation. The potential for exploiting this technique to produce rolling direction texture for anisotropic properties is also discussed. © *2009 American Institute of Physics*. [DOI: 10.1063/1.3138782]

Pulsed, melt-mediated laser crystallization techniques have been studied extensively for a range of material classes including semiconductors and elemental and alloyed metals.[1–3] The process provides a flexible means for spatial control over the presence of crystalline/amorphous regions as well as very precise control over the resulting microstructure itself. Silicon thin films have been processed in this manner for the production of thin film transistors for use in active matrix displays (e.g., liquid crystal display and organic light emitting diode). These applications also rely on the ability of the process for controlling the density of microstructural defects (e.g., high-angle grain boundaries), which have significant effects on device performance.[4] Additionally, advanced techniques such as the so-called sequential lateral solidification (SLS) processes first developed by Sposili and Im[5] implement successive position-controlled irradiations to grow extremely long (directional SLS) or periodically aligned elongated (two-shot SLS) crystals resulting in strong growth or rolling direction (RD) preferred orientations.

Several investigations on the use of laser annealing in order to control the spatial extents of crystalline regions have been conducted, although they have all been restricted to continuous-wave (cw), solid phase processing. Wang *et al.*[6] and Bellouard and co-workers[7] used a near IR cw laser to selectively solid-phase crystallize a sputter deposited NiTi thin film. He *et al.*[8] investigated the use of a cw CO_2 laser to selectively anneal a NiTi thin film via solid-phase crystallization as well.

This work utilizes pulsed, melt-mediated laser crystallization techniques to generate laterally grown, large aspect ratio NiTi crystals. Since shape memory responses stem from well-defined crystallographic shifts, both the shape memory and superelastic effects are anisotropic. Liu and Zheng[9] reported on the anisotropic effects associated with recoverable stress/strain as well as the constrained recovery attributes associated with the shape memory and superelastic effects respectively. The ultimate goal of this effort is to generate directionally grown crystals with highly preferred RD texture for microscale diaphragmatic actuation devices. Controlling the RD angle of alignment relative to the actuation axes has significant implications for actuation optimization in terms of frequency response and work output.

Amorphous NiTi films were deposited by simultaneous cosputtering from an alloyed NiTi target and pure titanium target at powers of 302 and 50 W, respectively, for 300 s at an argon pressure of 3 mTorr resulting in films 200 nm in thickness. The films were deposited on a 1 μm ultralow residual stress (<50 MPa) silicon nitride (Si_3N_4) barrier layer that had been deposited on a [100] silicon wafer via low pressure chemical vapor deposition. The film composition was obtained as Ni-52.4 at. % via a calibrated electron microprobe.[10]

Films were single-shot, pulse irradiated by a 308 nm wavelength, XeCl excimer laser with 30 ns pulse duration over a wide range of incident laser energy densities. Energy density was uniform within the irradiated region whose geometry was a square, 320×320 μm^2. The laser system is synchronized with the underlying *XYZ* motion system such that a series of energy densities may be applied producing a spatial array on a single specimen. The reader is directed to Birnbaum *et al.*,[11] which investigated the effects of substrate temperature on the resulting film microstructure and phase as well as the shape memory response (or lack thereof) in laser processed films. This work confirms the films were indeed crystallized via x-ray diffraction with a fully austenitic composition for films irradiated at 800 °C substrate temperatures. Furthermore, nanoindentation of these films demonstrated a superelastic response, consistent with the austenitic phase of NiTi.

Lateral growth at the boundary of irradiation is possible when complete, through film thickness melting occurs. Upon complete melting, solidification occurs via two distinct pathways: nucleation and growth, and lateral growth of unmelted crystalline seeds. Away from the irradiated boundary, supercooling of the film is required for nucleation (homogeneous or heterogeneous) and growth of planar, equiaxed, so-called "pancake" grains. Figure 1 is an electron micrograph depicting a film that has undergone complete melting and reveals the presence of both lateral growth at the boundary of irra-

a)Electronic mail: andrew.birnbaum@gmail.com.

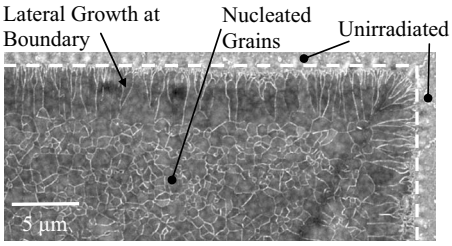

FIG. 1. Scanning electron microscopy image of the corner region of the flood irradiated area. The dotted line depicts the boundary of irradiation where lateral crystal growth occurs from unmelted seeds.

diation, and nucleated grains toward the interior of the irradiated region. As opposed to the nucleated grains where supercooling is required, unmelted seeds will grow into the adjacent molten regions upon reaching temperatures fractions of a degree centigrade below the equilibrium melting temperature. Therefore, upon cooling, lateral growth begins prior to nucleation away from the boundary. Lengths are therefore limited by the lateral growth velocity and the time required (necessary degree of supercooling and temporal

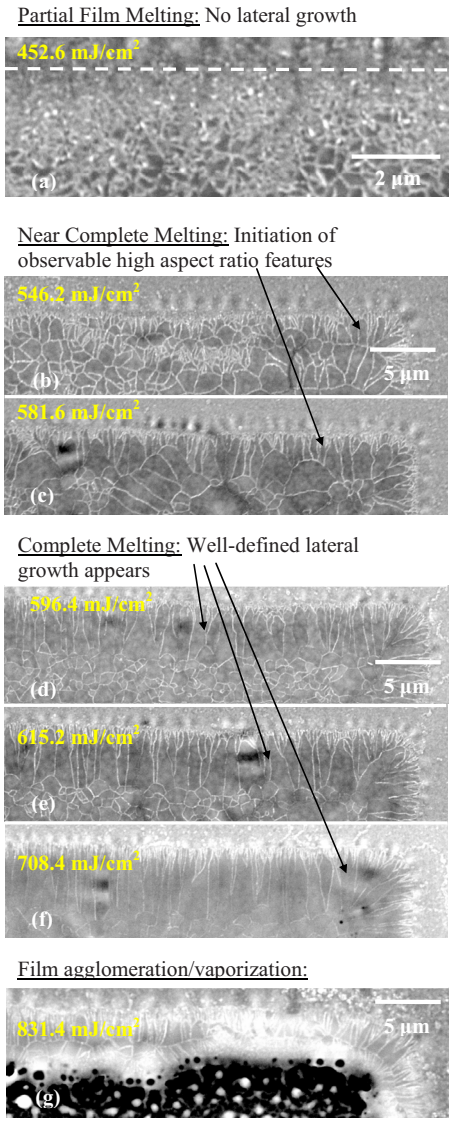

FIG. 2. (Color online) [(a)–(g)] Electron micrographs of laterally grown crystals at the boundary of irradiation for a series of incident laser energy densities.

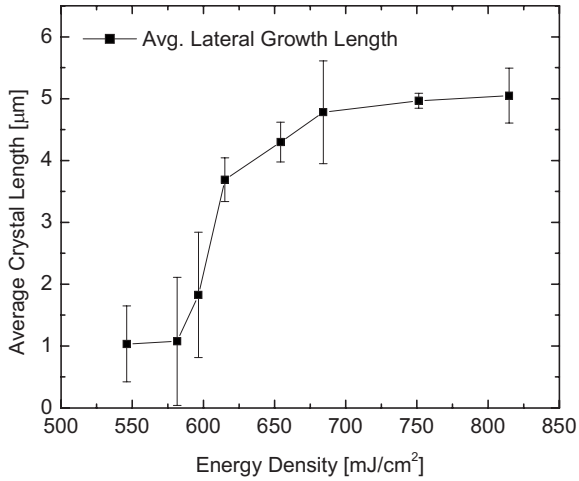

FIG. 3. Plot of average lateral growth length as a function of incident laser energy density, $T_{substrate}$=800 °C. Note the rapid increase in length upon complete, through thickness melting.

temperature gradient) for nucleation and growth to occur. Lateral growth is arrested upon impingement of nucleated grains.

Initial attempts at generating laterally grown crystals at room temperature proved unsuccessful (Birnbaum *et al.*[11]) upon microstructural examination (not shown). It was observed that there were in fact features resembling lateral growth, however, due to the rate with which solidification occurred, the crystals were not long enough (<1 μm) for implementation of the SLS process.

This reduced/ill-defined lateral growth is believed to have stemmed from one of two or both of the following factors. The first issue being the fact that the film is amorphous, as-deposited. Thus it is not well understood how lateral growth can proceed from the boundary if there are no pre-existing crystals to act as seeds for growth. One potential explanation is that solid phase crystallization occurs near the boundary, as temperatures just below the melting temperature will be reached. The other factor is the growth rate from the seeds. In order to suppress the nucleation and growth process away from the irradiated boundaries, an elevated substrate temperature, $T_{substrate}$=800 °C, was maintained in conjunction with a controlled argon atmosphere in order to mitigate the effects of film oxidation. As will be seen below, the 800 °C substrate temperature does indeed facilitate the growth of well defined lateral features (Fig. 1). Additionally, as the specimen is located within a hot stage enclosure, it was also necessary to laser process transmissively through a quartz window. Heating the film prior to irradiation resulted in solid phase crystallization *prior* to irradiation, thus addressing both potential issues of pre-existing seeds *and* reducing the temporal temperature gradient.

Figures 2(a)–2(g) are a series of electron micrographs of the boundary region of irradiated areas for a series of increasing laser energy densities at elevated substrate temperature. This series of micrographs reveals the emergence of lateral growth at the boundary as the energy density increases and becomes sufficient for complete film melting. Figure 3 is a compilation of the average lateral growth lengths as a function of energy density. Figure 2(a) shows a portion of film that has been processed at 452.6 mJ/cm^2. The white dashed line is the boundary of irradiation. Clearly

no lateral growth is present and the average grain diameter is of the order of the film thickness; both characteristics indicative of processing in the partial melting regime. Since the film has only been partially melted through the thickness, solidification proceeds via vertical epitaxial regrowth, thus preventing lateral growth into the melt from boundary seeds. As the laser energy density increases, lateral crystals begin to appear, although in a nonuniform manner and of a reduced length. This behavior is indicative of operating in the *near complete melting* regime[11] and occurs over energy densities through which partial melting transitions to complete melting. Due to local inhomogeneities, which may come from laser energy density, film thickness, microstructue, or whatever reasons, some grains could remain whereas the other portion of films are completely melted. The molten portions of the film go through nucleation and growth, while the remained seeds grow immediately upon reaching only slight undercoolings resulting in a bimodal grain size distribution with relatively small nucleated grains and large regrown grains from the remained seeds (average grain diameter ~ 3 μm). Finally, it is seen that upon irradiating near 600 mJ/cm^2, uniform lateral growth is observed. This behavior is manifested as a sudden increase in the average lateral growth length upon reaching the complete melt threshold CMT due to the fact that there is now a completely molten volume available to the adjacent unmelted crystals for growth. This lateral growth is also accompanied by nucleation and growth of crystals away from the boundary (average grain diameter $\sim$800 nm). Birnbaum *et al.*[11] provides a complete description of the microstructure away from the boundary area. Furthermore, it is observed that the average length continues to increase monotonically until the incident energy reaches approximately 830 mJ/cm^2 resulting in agglomeration and/or vaporization [Fig. 2(g)]. The nature of the development of lateral growth presented here in terms of the progression through melting regimes for NiTi is consistent to that observed in the Si thin films.[2]

Lateral growth of thin film NiTi crystals was demonstrated via the utilization of a pulsed, melt-mediated laser crystallization technique. The crystals produced were of sufficient length such that the SLS process may be implemented. Such work will benefit the microfabrication of NiTi-based devices with controllable microstructures. Further efforts will go toward characterization of RD texture via electron backscatter diffraction (EBSD) as well as integration in to a thin film diaphragmatic shape memory actuator.

[1]T. Sameshima and S. Usui, Mater. Res. Soc. Symp. Proc. **71**, 435 (1986).
[2]J. S. Im, H. J. Kim, and M. O. Thompson, Appl. Phys. Lett. **63**, 1969 (1993).
[3]C. J. Lin and F. Spaepen, Acta Metall. **34**, 1367 (1986).
[4]J. S. Im, M. A. Crowder, R. S. Sposili, J. P. Leonard, H. J. Kim, J. H. Yoon, V. V. Gupta, and H. Jin Song, and Cho, Phys. Status Solidi A **166**, 603 (1998).
[5]R.S. Sposili and J.S. Im, Appl. Phys. Lett. **69**, 2864 (1996).
[6]X. Wang, Y. Bellouard, and J. J. Vlassak, Acta Mater. **53**, 4955 (2005).
[7]Y. Bellouard, T. Lehnert, J. E. Bidaux, T. Sidler, R. Clavel, and R. Gotthardt, Mater. Sci. Eng., A **273–275**, 795 (1999).
[8]Q. He, M. H. Hong, W. M. Huang, T. C. Chong, Y. Q. Fu, and H. J. Du, J. Micromech. Microeng. **14**, 950 (2004).
[9]Y. Liu, and Q.S. Zheng, Phil. Mag. A **82**, 665 (2002).
[10]H. J. Lee and A. G. Ramirez, Appl. Phys. Lett. **85**, 1146 (2004).
[11]A. J. Birnbaum, U. J. Chung, X. Huang, J. S. Im, A. G. Ramirez, and Y. L. Yao, J. Appl. Phys. **105**, 073502 (2009).